

# Trap analysis on Pt-AlGa<sub>N</sub>/Ga<sub>N</sub> Schottky barrier diode through deep level transient spectroscopy

Ashish Kumar<sup>1,2,†</sup>, Jayjit Mukherjee<sup>3</sup>, D. S. Rawal<sup>3</sup>, K. Asokan<sup>2</sup>, and D. Kanjilal<sup>2</sup>

<sup>1</sup>Department of Physics, School of Natural Science, University of Petroleum and Energy Studies, Bidholi, Dehradun - 248007, India

<sup>2</sup>Inter University Accelerator Centre, Aruna Asaf Ali Road, Vasantkunj, New Delhi - 110067, India

<sup>3</sup>Solid State Physics Laboratory, DRDO, Timarpur, New Delhi - 110054, India

**Abstract:** Trap characterization on Ga<sub>N</sub> Schottky barrier diodes (SBDs) has been carried out using deep-level transient spectroscopy (DLTS). Selective probing by varying the ratio of the rate window values ( $r$ ) incites different trap signatures at similar temperature regimes. Electron traps are found to be within the values: 0.05–1.2 eV from the conduction band edge whereas the hole traps 1.37–2.66 eV from the valence band edge on the SBDs. In the lower temperature regime, the deeper electron traps contribute to the capacitance transients with increasing  $r$  values, whereas at the higher temperatures >300 K, a slow variation of the trap levels (both electrons and holes) is observed when  $r$  is varied. These traps are found to be mainly contributed to dislocations, interfaces, and vacancies within the structure.

**Key words:** deep traps; Pt-SBD; DLTS; rate window; defects

**Citation:** A Kumar, J Mukherjee, D S Rawal, K Asokan, and D Kanjilal, Trap analysis on Pt-AlGa<sub>N</sub>/Ga<sub>N</sub> Schottky barrier diode through deep level transient spectroscopy[J]. *J. Semicond.*, 2023, 44(4), 042802. <https://doi.org/10.1088/1674-4926/44/4/042802>

## 1. Introduction

Gallium nitride has proved to be a superior material due to its advanced qualities like high bandgap and high thermal conductivity<sup>[1, 2]</sup>. These advantages over other conventional semiconductors have led Ga<sub>N</sub> to be used in multiple applications in power electronic devices, optoelectronics as in LEDs, LASERS, photo-detectors, and solar cells<sup>[3–6]</sup>. The AlGa<sub>N</sub>/Ga<sub>N</sub> heterojunction with inherent interface polarization leads to high mobilities and high saturation velocities in 2D electron gas (2DEG) at interface and is most suitable for high-frequency applications. Despite all the above application advantages, Ga<sub>N</sub> systems also face reliability issues due to the presence of defects/traps within the epitaxial layers and at the interfaces<sup>[7, 8]</sup>.

The heterostructure used for devices fabrication plays a crucial role in governing the device characteristics. Epitaxial growth on lattice-mismatched substrates leads to tensile and compressive strains which lead to dislocations and extended defects. Furthermore, the AlGa<sub>N</sub>/Ga<sub>N</sub> interface may also house interface states which readily modulate the 2DEG concentration at the interface and results in degraded device performance. Micro and optoelectronic devices require a defect-free surface, an active layer immune to any dislocation/defect beneath it, and a good crystalline quality material. It is reported that the charge imbalance caused due to carrier trapping by defects leads to high leakage currents<sup>[9]</sup>, breakdown<sup>[10]</sup>, current collapse in HEMTs<sup>[11]</sup>, and reduced quantum efficiency in light-emitting diodes<sup>[12]</sup>. The aforementioned material superiority of Ga<sub>N</sub> has led to widespread research for

power applications. A vast of the reported work has utilized a Ni-based metal scheme for the gate contact<sup>[13–18]</sup>. However, the leakage in the devices can be improved by using higher work function metals for the gate contact. Pt having a work function of 5.65 eV<sup>[19]</sup> has been reported having a higher barrier height<sup>[20]</sup> as compared to conventional Ni/Au gate contacts on Ga<sub>N</sub>-based devices. Enhanced barrier height has also been achieved through annealing of the Schottky contact<sup>[21–23]</sup>. Apart from conventional nitride passivation, the surface states can also be mitigated through Ru or sulphide-based schemes<sup>[24, 25]</sup>. Thereby characterization of these defects is important towards the development of reliable Ga<sub>N</sub> devices. Detailed trap signature studies of Ga<sub>N</sub> with Pt-Schottky contacts are not available in the reported literature and needs to be studied using reliable technique for stable Ga<sub>N</sub> device operation in power/RF electronics. Deep level transient spectroscopy (DLTS)<sup>[26]</sup> offers substantial advantages over other characterization techniques<sup>[23, 27, 28]</sup> to study deep trap states which are not easily obtained from other conventional methods.

In this article, we have analyzed Pt-AlGa<sub>N</sub>/Ga<sub>N</sub> Schottky barrier diode (SBD) on sapphire using deep level transient spectroscopy (DLTS) throughout a temperature range of 150–480 K. The variation of the ratio of the rate windows reveals numerous trap signatures within the device throughout the observed temperature range and enables selective probing of deep traps present within the epitaxial layers. A higher temperature regime has been probed for the wide band gap material and the findings provide all the possible trap signatures that may be introduced into Ga<sub>N</sub> systems which can have detrimental impact on device performance. This helps to expand the understanding of the traps originating from extended defects and interface states and how traps respond in different temperature regimes.

Correspondence to: A Kumar, [ashish.kumar@ddn.upes.ac.in](mailto:ashish.kumar@ddn.upes.ac.in),  
[dr.akmr@gmail.com](mailto:dr.akmr@gmail.com)

Received 19 OCTOBER 2022; Revised 25 NOVEMBER 2022.

©2023 Chinese Institute of Electronics

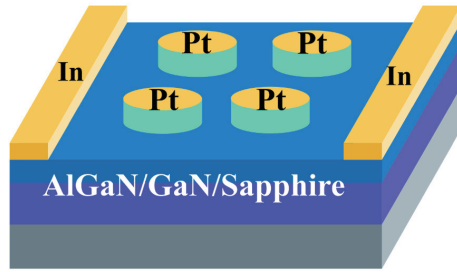


Fig. 1. (Color online) Schematic of the Pt-AlGaIn/GaN SBD under experimentation.

## 2. Experimental details

The SBDs were fabricated on commercially procured Al-GaN/GaN heterostructure grown on the sapphire substrate by metal-organic chemical vapor deposition (MOCVD) technique. Circular platinum (Pt) dots (1.5 mm diameter, 100 nm thickness) were deposited using a metal mask in an ultra-high vacuum chamber followed by Indium (In) metal strips deposited at opposite edges for ohmic contacts as shown in the schematic diagram in Fig. 1. DLTS characterization was done by a conventional boxcar method comprised of a capacitance meter (Boonton 7200), a pulse generator (HP 8012B), temperature controller (Lakeshore 340), ADC digitizer (DAQ card NI PCI 6251), and a computer interfaced with LabVIEW software. A temperature range of 150–480 K was used for the DLTS spectrum with a voltage excitation of 10 V (square pulse) applied on the SBD. The setup of the DLTS instrumentation is schematically shown in Fig. 2. The filling and emptying pulse-width were kept at 2 and 10 ms respectively with a pulse sampling rate of 50 ms. The DLTS signal was captured by sampling capacitance transient data at different time intervals in the range of 5  $\mu$ s to 9 ms. As demonstrated by Lang<sup>[26]</sup>, the DLTS signal is generated from the difference in the  $C(t)$  spectrum (Eq. (1)) for two sampling times ( $t_1$  and  $t_2$ ) defined by a rate window ( $t_1 - t_2$ ) utilizing a double boxcar integrator.

$$C(t) = C_0 \left[ 1 - \frac{N_T}{2N_D} \exp\left(-\frac{t}{\tau_e}\right) \right]. \quad (1)$$

Here,  $C_0$  is the zero-bias capacitance,  $N_T$  is the trap concentration, and  $N_D$  is the donor concentration. When the temperature ( $T$ ) is varied, the time constant ( $\tau_e = \frac{1}{e_n}$ ) corresponding to a particular trap changes, this leads to a maximum in the DLTS signal as obtained from the capacitance transients. For different sampling times (rate windows), a specific value of  $\tau_{e,\max}$  is obtained (Eq. (2)). These values are used to generate the Arrhenius plot following Eq. (3), from which the trap activation energy ( $E_a$ ) can be calculated.

$$\tau_{e,\max} = \frac{t_2 - t_1}{\ln(t_2/t_1)}, \quad (2)$$

$$\frac{e_n}{T^2} = \gamma_n \sigma_n \exp\left(\frac{-E_a}{\kappa_B T}\right), \quad (3)$$

where  $\kappa_B$  is the Boltzmann constant,  $\sigma_n$  is the trap concentration,  $\gamma_n = (v_{th}/T^{1/2})(N_C/T^{3/2})$  with  $v_{th}$  as the thermal velocity and  $N_C$  as the effective density of states. The DLTS analysis results

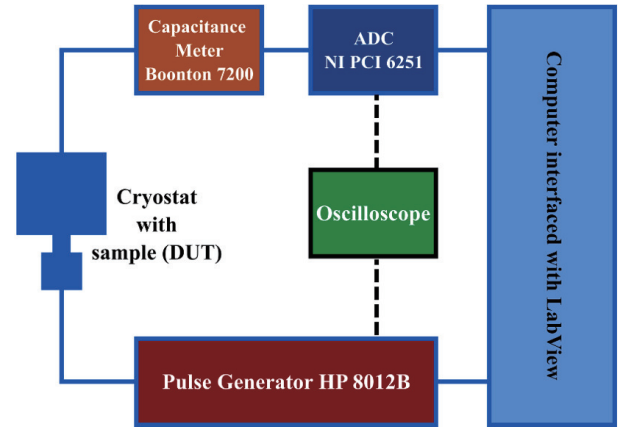


Fig. 2. (Color online) DLTS setup used for the experimentation.

have been presented for four rate window ratios  $r = t_2/t_1$  ( $= 2, 3, 5$  and  $10$ ) to get the maximum number of trap signatures in the SBDs. For the analysis, we have chosen the positive peaks in the DLTS signal for the electron traps as per the convention (which was preset from the experimental setup). The DLTS spectra is a result of multiple trap signatures (since any change in trap occupancy is directly reflected in the capacitance), hence multiple peaks correspond to multiple traps. Thus, the peaks were deconvoluted and analyzed with gaussian fitting function to determine the peak positions for a particular trap.

## 3. Results and discussion

The DLTS spectra for  $r = 2$  are presented in Fig. 3(a) for different  $t_1$  values between (10–150 ms). A positive peak  $P_1^2$  at around 330 K for high  $t_1$  values and for 10 ms is observed. Along with it, a negative peak  $P_2^2$  around 400 K is also observed for high  $t_1$  values. The activation energies calculated from the Arrhenius plots are shown in Fig. 3(b). The  $P_1^2$  peak corresponds to an electron trap  $E_C - 0.87$  eV and the  $P_2^2$  extracts a hole trap of  $E_V + 1.56$  eV. The electron trap peak  $P_1^2$  decreases with increasing  $t_1$  values whereas the hole trap peak  $P_2^2$  appears for  $t_1 = 50$  ms and remains constant till 250 ms. A similar deep-level electron trap in GaN ( $P_1^2$ ) has been ascribed to nitrogen interstitials ( $N_i$ ) and observed in low C-doped SBDs and high quality GaN films. Various studies have also shown yellow luminescence in GaN originating from trap centres with similar activation energies (0.75 to 0.89 eV)<sup>[29–31]</sup>.

Next, Fig. 4 shows DLTS analysis for rate window ratio  $r = 3$ , where three traps are evident: two-electron traps  $P_1^3, P_2^3$ , and a hole trap  $P_3^3$ . All the evident traps are identified for  $t_1$  values  $> 50$  ms and the peaks gradually decrease for  $t_1 = 200$  ms shown in Fig. 4. The trap peak  $P_1^3$  is a shallow level around 0.05 eV from the conduction band edge. In contrast to other traps evaluated with this rate window, the trap peak moves towards lower temperatures with increasing  $t_1$ . Shallow trap levels around  $E_C - 0.04$  eV originate due to open core dislocations within the crystal structure<sup>[32, 33]</sup>. The  $P_2^3$  is a deep trap with an activation energy of 1 eV. This trap was also evident from DLTS on GaN-based SBDs with thin GaN layers and are generally associated with threading dislocations<sup>[34]</sup>. The hole trap  $P_3^3$  with the energy level of  $E_V + 1.37$  eV peaks around 400 K. Deep hole traps similar to  $P_3^3$  have been previously reported to be present in the AlGaIn/GaN heterointerface from

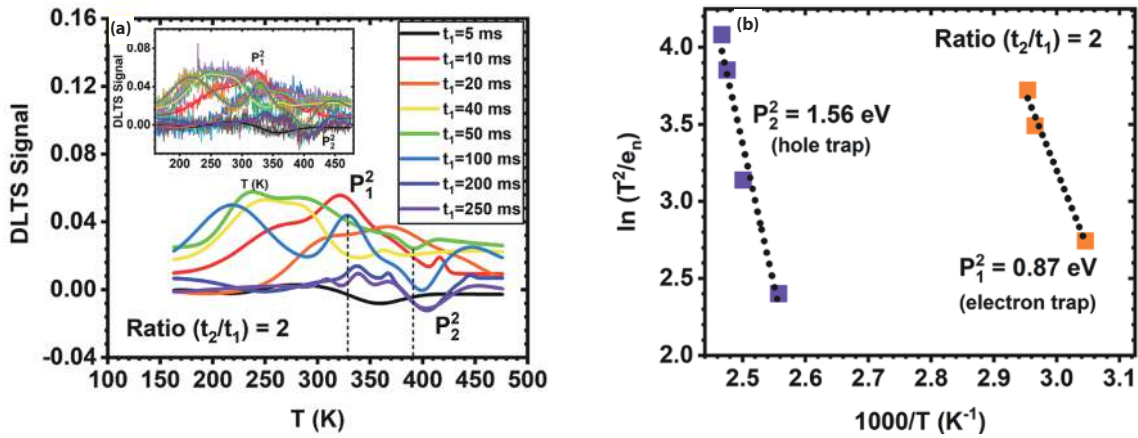


Fig. 3. (Color online) (a) DLTS signal for  $r = 2$  with  $t_1$  ranging from 10–150 ms. The vertical dashed lines are the peak position as they appear in the spectra for the first instance of sampling time. The inset shows the gaussian fit with the experimental data. (b) Calculated activation energies for the two peaks as denoted by  $P_1^2$  and  $P_2^2$ .

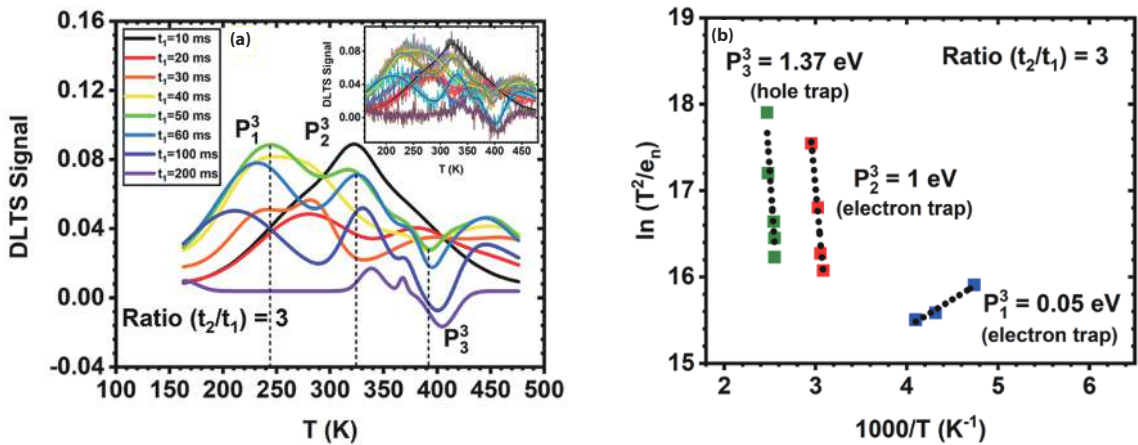


Fig. 4. (Color online) (a) DLTS signal for  $r = 3$  with  $t_1$  ranging from 10–200 ms. The vertical dashed lines are the peak position as they appear in the spectra for the first instance of sampling time. The inset shows the fit with the experimental data. (b) Calculated activation energies for trap peaks  $P_1^3$ ,  $P_2^3$ , and  $P_3^3$ .

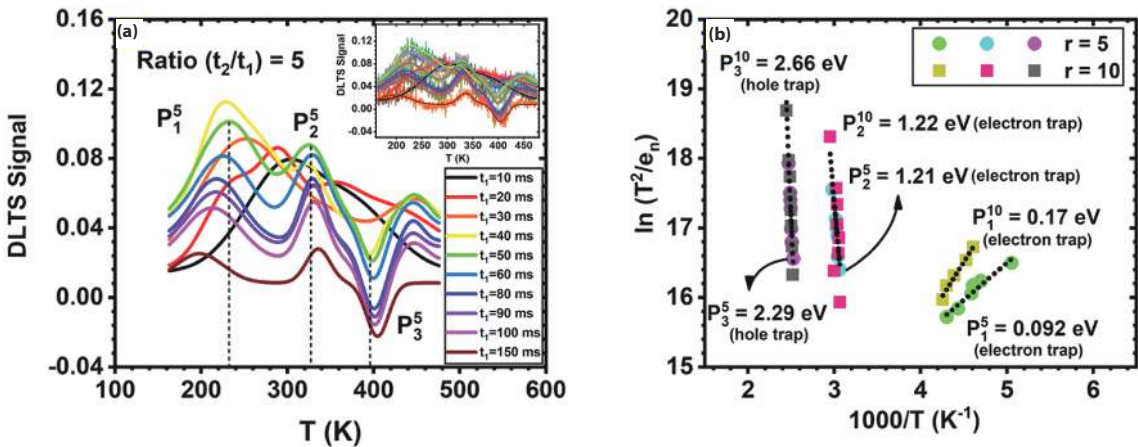


Fig. 5. (Color online) (a) DLTS signal for  $r = 5$  for  $t_1 = 10$ –150 ms. The vertical dashed lines are the peak position as they appear in the spectra for the first instance of sampling time. The inset shows the fit with the experimental data. (b) Calculated activation energies for the trap peaks for  $r = 5$  and  $r = 10$ .

DLTS studies<sup>[35, 36]</sup> and the same is to be accounted in this experiment as the SBDs are fabricated on AlGaIn/GaN heterostructure.

The rate window  $r = 5$  reveals three trap levels (Fig. 5(a)) with one shallow electron peak ( $P_1^5$ ), a deep electron peak ( $P_2^5$ ), and a deep hole peak ( $P_3^5$ ). The  $w_1^5$  trap of  $E_C - 0.09$  eV has

been reported as a native defect in n-GaN due to nitrogen vacancies ( $V_N$ ) leading to shallow levels around 100 meV<sup>[37]</sup>. Apart from pristine GaN SBDs, a similar trap level was reported in n-GaN SBDs after undergoing cumulative doses of  $^{60}\text{Co}$ - $\gamma$ -radiation<sup>[38]</sup>. The heavy ion irradiation on GaN SBDs facilitates defect formation as reported in Refs. [39, 40]. The de-

Table 1. Summary of the electron and hole traps from the DLTS experimentation.  $E_a$  is the activation energy of the trap measured from the conduction ( $E_C$ ) or valence band ( $w_V$ ) edge, and  $N_T$  is the trap density as calculated from the Arrhenius plots.

Ratio ( $r$ )	Trap peak, nature	$E_a$ (eV)	$N_T$ ( $10^{16} \text{ cm}^{-3}$ )	Remark	Ref.
2	$P_1^2, e$	$E_C - 0.87$	2.05	Nitrogen interstitial ( $N_i$ )	[29–31]
	$P_2^2, h$	$E_V + 1.56$	1.03		
3	$P_1^3, e$	$E_C - 0.05$	5.14	Open core dislocation	[32, 35]
	$P_2^3, e$	$E_C - 1.00$	3.08	Threading dislocations	[34]
	$P_3^3, h$	$E_V + 1.37$	1.17	AlGaIn/GaN interface	[35,36]
5	$P_1^5, e$	$E_C - 0.09$	4.41	Nitrogen vacancies	[37, 38, 41]*
	$P_2^5, e$	$E_C - 1.21$	3.23	Extended defects in GaN	[35, 36]
	$P_3^5, h$	$E_V + 2.29$	1.54	Ga-vacancy/N-antisite	[44]
10	$P_1^{10}, e$	$E_C - 0.17$	2.82	Bulk GaN/interface states	[45, 46]
	$P_2^{10}, e$	$E_C - 1.22$	2.79	Extended defects in GaN	[35, 36]
	$P_3^{10}, h$	$E_V + 2.66$	1.45	Point/extended defects	[47]

\*This trap level was also evident after e/ $\gamma$ -irradiation on GaN SBDs.

fects have been explained to be generated from N vacancies when energetic radiation/electrons on collision with GaN surface create either  $V_N-N_i$  Frenkel pairs and/or defects composed of longer chains<sup>[41, 42]</sup>. Deep electron trap like  $P_2^5$  around 1.2 eV has been correlated to extended defects in bulk GaN<sup>[35]</sup> as well as electron-irradiated SBDs<sup>[43]</sup>. A deep hole trap,  $P_3^5 = E_V + 2.29$  eV peaking around 400 K is also observed. The spectrally resolved measurement reveals a trap centered around 2.27 eV from the valence band edge ( $E_V$ )<sup>[44]</sup> possibly from gallium vacancy ( $V_{Ga}$ ) or nitrogen antisite ( $N_{Ga}$ ). This trap is found to be responsible for optical quenching-related anomalous dispersion of off-state leakage current under illumination in GaN HEMT.

Higher ratios lead to deeper trap states being resolved through DLTS as shown in Fig. 5(b). We observed a shallow electron trap  $P_1^{10}$  of 0.17 eV which has been discussed in Refs. [45, 46] reportedly around  $E_C - 0.18$  eV, originates from bulk GaN and/or interface states in AlGaIn/GaN HEMTs. The  $P_2^{10}$  electron trap exactly reciprocates the  $P_3^5$  trap as obtained earlier centered around 325 K. The deep hole trap  $P_3^{10}$  has an energy level of  $E_V + 2.66$  eV. This is also consistent with Armstrong<sup>[47]</sup> who has reported a high-density deep hole trap around 2.59 eV from valence band edge for InGaIn/GaN heterostructures from deep level optical spectroscopy (DLOS) studies. They ascribed this to most likely point or extended defects in In-GaN underlayers. The summary of all the trap states as extracted from the DLTS analysis is presented in Table 1 along with the trap properties.

From the trap signatures as a result of extensive experimentation, it is evident that by increasing the ratio ( $r$ ) of the rate windows ( $t_1, t_2$ ) different traps corresponding to similar temperature regimes were evaluated as shown in Fig. 6. For this, we focus on the three most dominant trap peaks as evident in the DLTS spectra for different  $r$ -values. The temperature range is divided into three regions. Region I (<250 K) is predominantly characterized by shallow electron traps and an increase in the trap energy level is observed as  $r$  is increased. It is also interesting to note that for all the evaluated shallow levels for different rate windows ( $P_1^3, P_1^5$  and  $P_1^{10}$ ), the DLTS peaks shift to lower temperatures with increasing  $t_1$  values. This leads to obtaining shallow electron traps in a lower tem-

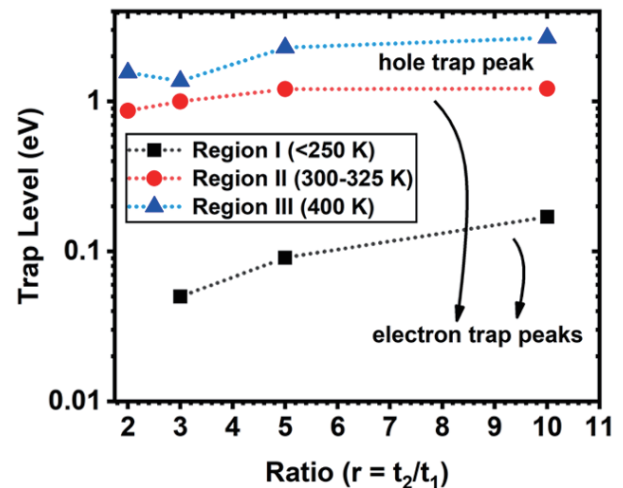


Fig. 6. (Color online) Trap energy levels from DLTS for different ratios of the rate windows. The energy level corresponds to the offset from conduction band edge ( $E_C$ ) for electron traps and from valence band edge ( $E_V$ ) for hole traps.

perature regime with different dynamics as compared to the other deep levels. The trap peaks in region II (300–350 K) correspond to deep traps and become invariant revealing a constant electron trap of  $E_C - 1.2$  eV for  $r = 5$  and 10. The hole trap peaks observed in region III (around 400 K) show a non-monotonic increase in energy values with 2.66 eV for  $r = 10$ . The higher  $r$ -value helps to find traps with larger time constants and thereby deep trap states within the heterostructure, which is evident from the traps in regions I and III. This leads to the selective probing of traps being evident in different temperature regimes.

#### 4. Conclusion

Present investigation on Pt-AlGaIn/GaN SBDs through DLTS has revealed various electron and hole trap levels. In the analysis, the number of trap peaks observed also changes with the  $r$  value with higher  $r$ -values revealing a greater number of trap peaks. It was also observed that traps originating from different defect centers respond in similar temperature regimes. This can be used for selective probing of electron and

hole traps. The trap levels are compared to those reported earlier which are attributed to dislocations, AlGaN/GaN interface, and vacancy defects within the epitaxial layers. The above results from this extensive DLTS experimentation reveal a wide view of the trap signatures in GaN systems.

## Acknowledgements

A.K. would like to acknowledge the financial support received from the Department of Science and Technology, India through DST-INSPIRE Faculty scheme (DST/INSPIRE/04/2015/001572).

## References

- [1] Mishra U K, Parikh P, Wu Y F. AlGaN/GaN HEMTs—an overview of device operation and applications. *Proc IEEE*, 2002, 90, 1022
- [2] Millán J, Godignon P, Perpiñà X, et al. A survey of wide bandgap power semiconductor devices. *IEEE Trans Power Electron*, 2014, 29, 2155
- [3] Davis R F. III-V nitrides for electronic and optoelectronic applications. *Proc IEEE*, 1991, 79, 702
- [4] Yu H B, Memon M H, Wang D H, et al. AlGaN-based deep ultraviolet micro-LED emitting at 275 nm. *Opt Lett*, 2021, 46, 3271
- [5] Yu H, Memon M H, Jia H, et al. A 10 x 10 deep ultraviolet light-emitting micro-LED array. *J Semicond*, 2022, 43, 062801
- [6] Wang D H, Wu W T, Fang S, et al. Observation of polarity-switchable photoconductivity in III-nitride/MoS<sub>x</sub> core-shell nanowires. *Light Sci Appl*, 2022, 11, 227
- [7] Asghar M, Muret P, Beaumont B, et al. Field dependent transformation of electron traps in GaN p-n diodes grown by metal-organic chemical vapour deposition. *Mater Sci Eng B*, 2004, 113, 248
- [8] Moroz V, Wong H Y, Choi M, et al. The impact of defects on GaN device behavior: Modeling dislocations, traps, and pits. *ECS J Solid State Sci Technol*, 2016, 5, P3142
- [9] Usami S, Ando Y, Tanaka A, et al. Correlation between dislocations and leakage current of p-n diodes on a free-standing GaN substrate. *Appl Phys Lett*, 2018, 112, 182106
- [10] Saito W, Kuraguchi M, Takada Y, et al. Influence of surface defect charge at AlGaIn-GaN-HEMT upon Schottky gate leakage current and breakdown voltage. *IEEE Trans Electron Devices*, 2005, 52, 159
- [11] Ghosh S, Das S, Dinara S M, et al. Off-state leakage and current collapse in AlGaIn/GaN HEMTs: a virtual gate induced by dislocations. *IEEE Trans Electron Devices*, 2018, 65, 1333
- [12] Lee I H, Polyakov A Y, Smirnov N B, et al. Changes in electron and hole traps in GaN-based light emitting diodes from near-UV to green spectral ranges. *Appl Phys Lett*, 2017, 110, 192107
- [13] Shiojima K, Suemitsu T, Ogura M. Correlation between current-voltage characteristics and dislocations for n-GaN Schottky contacts. *Appl Phys Lett*, 2001, 78, 3636
- [14] Saito W, Takada Y, Kuraguchi M, et al. Recessed-gate structure approach toward normally off high-voltage AlGaIn/GaN HEMT for power electronics applications. *IEEE Trans Electron Devices*, 2006, 53, 356
- [15] Saadat O I, Chung J W, Piner E L, et al. Gate-first AlGaIn/GaN HEMT technology for high-frequency applications. *IEEE Electron Device Lett*, 2009, 30, 1254
- [16] Lee F, Su L Y, Wang C H, et al. Impact of gate metal on the performance of p-GaN/AlGaIn/GaN high electron mobility transistors. *IEEE Electron Device Lett*, 2015, 36, 232
- [17] Kumar A, Mahajan S, Vinayak S. Studies on the thermal stability of Ni/n-GaN and Pt/n-GaN Schottky barrier diodes. *Mater Res Express*, 2016, 3, 085901
- [18] Huang Y P, Hsu W C, Liu H Y, et al. Enhancement-mode tri-gate nanowire InAlN/GaN MOSHEMT for power applications. *IEEE Electron Device Lett*, 2019, 40, 929
- [19] Lide D R. CRC handbook of chemistry and physics. Boca Raton: CRC Press, 2001
- [20] Wang L, Nathan M I, Lim T H, et al. High barrier height GaN Schottky diodes: Pt/GaN and Pd/GaN. *Appl Phys Lett*, 1996, 68, 1267
- [21] Jeon C M, Lee J L. Enhancement of Schottky barrier height on Al-GaN/GaN heterostructure by oxidation annealing. *Appl Phys Lett*, 2003, 82, 4301
- [22] Wang J, Zhao D, Sun Y, et al. Thermal annealing behaviour of Pt on n-GaN schottky contacts. *J Appl Phys*, 2003, 36, 1018
- [23] Kumar S, Gupta P, Guiney I, et al. Temperature and bias dependent trap capture cross section in AlGaIn/GaN HEMT on 6-in silicon with carbon-doped buffer. *IEEE Trans Electron Devices*, 2017, 64, 4868
- [24] Kumar A, Kumar M, Kaur R, et al. Barrier height enhancement of Ni/GaN Schottky diode using Ru based passivation scheme. *Appl Phys Lett*, 2014, 104, 133510
- [25] Kumar A, Singh T, Kumar M, et al. Sulphide passivation of GaN based schottky diodes. *Curr Appl Phys*, 2014, 14, 491
- [26] Lang D V. Deep-level transient spectroscopy: A new method to characterize traps in semiconductors. *J Appl Phys*, 1974, 45, 3023
- [27] Reshchikov M A, Morkoç H, Park S S, et al. Transient photoluminescence of defect transitions in freestanding GaN. *Appl Phys Lett*, 2001, 78, 2882
- [28] Bouya M, Malbert N, Labat N, et al. Analysis of traps effect on Al-GaN/GaN HEMT by luminescence techniques. *Microelectron Reliab*, 2008, 48, 1366
- [29] Reshchikov M, Shahedipour F, Korotkov R, et al. Deep acceptors in undoped GaN. *Phys B*, 1999, 273, 105
- [30] Reshchikov M A, Morkoç H. Luminescence properties of defects in GaN. *J Appl Phys*, 2005, 97, 061301
- [31] Belahsene S, Al Saqri N A, Jameel D, et al. Analysis of deep level defects in GaN pin diodes after beta particle irradiation. *Electronics*, 2015, 4, 1090
- [32] Venturi G, Castaldini A, Cavallini A, et al. Dislocation-related trap levels in nitride-based light emitting diodes. *Appl Phys Lett*, 2014, 104, 211102
- [33] Jones R, Elsner J, Haugk M, et al. Interaction of oxygen with threading dislocations in GaN. *Phys Status Solidi A*, 1999, 171, 167
- [34] Fang Z Q, Look D C, Kim D H, et al. Traps in AlGaIn/GaN/SiC heterostructures studied by deep level transient spectroscopy. *Appl Phys Lett*, 2005, 87, 182115
- [35] Fang Z Q, Claflin B, Look D C, et al. Deep traps in AlGaIn/GaN heterostructures studied by deep level transient spectroscopy: Effect of carbon concentration in GaN buffer layers. *J Appl Phys*, 2010, 108, 063706
- [36] Polyakov A Y, Lee I H. Deep traps in GaN-based structures as affecting the performance of GaN devices. *Mater Sci Eng R*, 2015, 94, 1
- [37] Boguslawski P, Briggs E L, Bernholc J. Native defects in gallium nitride. *Phys Rev B*, 1995, 51, 17255
- [38] Umana-Membreno G A, Dell J M, Hessler T P, et al. <sup>60</sup>Co gamma-irradiation-induced defects in n-GaN. *Appl Phys Lett*, 2002, 80, 4354
- [39] Kumar A, Kanjilal D, Kumar V, et al. Defect formation in GaN epitaxial layers due to swift heavy ion irradiation. *Radiation Effects and Defects in Solids*, 2011, 166, 739
- [40] Kumar A, Dhillion J, Verma S, et al. Identification of swift heavy ion induced defects in Pt/n-GaN Schottky diodes by in-situ deep level transient spectroscopy. *Semicond Sci Technol*, 2018, 33, 085008
- [41] Polenta L, Fang Z Q, Look D C. On the main irradiation-induced defect in GaN. *Appl Phys Lett*, 2000, 76, 2086
- [42] Look D C, Reynolds D, Hemsley J W, et al. Defect donor and acceptor in GaN. *Phys Rev Lett*, 1997, 79, 2273
- [43] Fang Z Q, Farlow G C, Claflin B, et al. Effects of electron-irradiation on electrical properties of AlGaIn/GaN Schottky barrier di-

- odes. *J Appl Phys*, 2009, 105, 123704
- [44] Das A, Ko D H, Lin R M, et al. Anomalous decrease of off-state drain leakage current in GaN/AlGaN HEMTs with dual optical excitation. *IEEE Electron Device Lett*, 2014, 35, 820
- [45] Mizutani T, Kawano A, Kishimoto S, et al. Drain current DLTS of normally-off AlGaIn/GaN HEMTs. *Phys Status Solidi C*, 2007, 4, 1536
- [46] Polyakov A Y, Smirnov N, Govorkov A, et al. Deep centers and persistent photocapacitance in AlGaIn/GaN high electron mobility transistor structures grown on Si substrates. *J Vac Sci Technol B*, 2013, 31, 011211
- [47] Armstrong A, Crawford M H, Koleske D D. Quantitative and depth-resolved investigation of deep-level defects in InGaIn/GaN heterostructures. *J Electron Mater*, 2011, 40, 369



**Ashish Kumar** is an Assistant Professor (research) at UPES Dehradun in physics department. He is a recipient of the SERB Research Scientist (2020), DST INSPIRE faculty award, and is an alum of the Lindau Nobel Laureate Meeting 2019, held at Lindau Germany. He earned his Ph.D. from Indian Institute of Technology Delhi in 2013. His research work focuses on areas of advanced semiconductor devices, HEMT and Schottky devices, power devices based on GaN, Ga<sub>2</sub>O<sub>3</sub>, SiC, and 2D materials. He carried out research in inorganic and organic thermoelectric generators.